This is a preprint, the final version is subject to change, of the American Mineralogist (MSA)
Cite as Authors (Year) Title. American Mineralogist, in press.
(DOI will not work until issue is live.) DOI: http://dx.doi.org/10.2138/am-2016-5707

Interface coupled dissolution-reprecipitation in garnet from subducted granulites and ultrahigh-pressure rocks revealed by phosphorous, sodium, and titanium zonation

Jay J. Ague[1,2] and Jennifer A. Axler[1]

[1]Department of Geology and Geophysics
Yale University
P.O. Box 208109
New Haven, CT 06520-8109 USA
jennifer.axler@yale.edu and jay.ague@yale.edu

[2]Peabody Museum of Natural History
Yale University
New Haven, CT 06511 USA

This is a preprint, the final version is subject to change, of the American Mineralogist (MSA)
Cite as Authors (Year) Title. American Mineralogist, in press.
(DOI will not work until issue is live.) DOI: http://dx.doi.org/10.2138/am-2016-5707

Abstract

Garnet zonation provides an unparalleled record of the pressure-temperature-time-fluid evolution of metamorphic rocks. At extreme temperature conditions >900 °C, however, most elements preserve little zonation due to intracrystalline diffusional relaxation. Under these conditions, slowly-diffusing trace elements including P, Na, and Ti have the best chance of recording metamorphic histories. Here we map dramatic zoning patterns of these elements in subducted high-pressure felsic granulite (Saxon Granulite Massif) and ultrahigh-pressure diamondiferous "saidenbachite" (Saxonian Erzgebirge, Bohemian Massif). The results show that garnet replacement via interface coupled dissolution-reprecipitation can strongly affect garnet compositions in subduction zones and that P, Na, and Ti record burial and exhumation histories that are otherwise lost to diffusion. In these samples, P diffuses the slowest, and Ti the fastest.

Introduction

Chemical zonation in garnet is widely used to reconstruct the pressure, temperature, time, and fluid histories of mountain belts. Most documented chemical zonation in garnet is the result of changing pressure-temperature-fluid conditions during growth as well as post-growth intracrystalline diffusion. In addition to diffusion, interface coupled dissolution-reprecipitation (ICDR) is another important process that can modify mineral compositions (e.g., Putnis and Austrheim, 2010; Harlov et al. 2011; Putnis and John, 2010). During ICDR, a disequilibrium fluid reacts with mineral surfaces, replacing the pre-existing composition with a new one that is likely to be in equilibrium with the fluid, although kinetic effects are also possible (e.g., Geisler et al. 2010). The interface between the old and new portions of the mineral is extremely sharp and propagates inward, leaving a zone of fluid-filled micro- or nano-porosity in its wake. Fresh reactants are transported to the reacting interface through the fluid-filled porosity, normally by

diffusion, whereas products are transported out. In this way, the interface advances until the entire crystal is replaced, commonly with little or no overall change in volume. Because diffusional transport occurs through a fluid phase, ICDR is in general much faster than intracrystalline diffusion. Successive episodes of ICDR can cross cut or replace earlier-formed replacement zones.

ICDR has been well-documented in minerals such as feldspar (e.g., replacement of albite by K-feldspar; e.g., Niedermeier et al. 2009) and zircon (Geisler et al. 2007; Rubatto et al. 2008). A growing body of evidence demonstrates that it can also play a significant role in garnet, as revealed by chemical and/or oxygen isotope zonation (e.g., Hames and Menard, 1993; Whitney et al. 1996; Alvarez et al. 2005; Pollock et al. 2008; Faryad et al. 2010; Martin et al. 2011; Page et al. 2013; Xu et al. 2013; Centrella et al. 2015; Chen et al. 2015). Nonetheless, the potential for trace element zonation to reveal ICDR processes remains relatively little explored.

Regardless of how garnet acquires zonation, at ultrahigh-temperature conditions >900 ^{o}C, diffusion for most elements is rapid and, thus, growth and recrystallization histories are largely erased. To have some chance of reconstructing these histories, the most slowly-diffusing elements must be identified. We focus on phosphorous, sodium, and titanium. Their concentrations in garnet generally increase with *P* and *T*, making their measurement via electron-probe microanalysis (EPMA) feasible (e.g., Hermann and Spandler, 2008; Auzanneau et al. 2010). Phosphorous, which substitutes mainly for Si^{4+} on tetrahedral sites, has been shown to preserve zoning in magmatic olivine (e.g., Mallmann et al. 2009) and garnet from amphibolite facies, near-UHT, UHT, and >900 ^{o}C ultrahigh-pressure (UHP) rocks (e.g., Spear and Kohn, 1996; Vielzeuf et al. 2005; Kawakami and Hokada, 2010; Kobayashi et al., 2011; Ague and Eckert, 2012; Axler and Ague, 2015a; 2015b; Jedlicka et al. 2015). Sodium substitution is linked

to P substitution in garnet by mechanisms such as $NaP\,M^{2+}_{-1}Si_{-1}$ (e.g., Hermann and Spandler, 2008), and complementary Na-P zonation patterns are documented for UHP rocks (e.g., Axler and Ague, 2015b). Titanium zonation tends to be somewhat smoother than that for P, but well-defined retrograde Ti-depletion halos surrounding rutile or ilmenite precipitates in garnet can be preserved in UHT and UHP garnets (e.g., Ague and Eckert, 2012; Axler and Ague, 2015b).

In this study, we use chemical maps to examine P, Na, and Ti zonation in subduction-related high-pressure (HP) eclogite facies granulite from the Saxon Granulite Massif (e.g., O'Brien, 2006; Rötzler et al. 2008) and UHP diamondiferous saidenbachite from the Saxonian Erzgebirge (e.g., Massonne, 2003). Our goals are to determine: (1) the nature and extent of zoning preservation and (2) what the implications of the zoning are for metamorphic processes. EPMA analyses were done using the JEOL-JXA8530F at Yale University; analytical methods are described in Axler and Ague (2015b). Element mapping employed 300 nA beam current and 200 ms dwell times. To avoid confusion, the abbreviation "P" is used only for phosphorous; pressure is written out in full except for the abbreviations "HP" and "UHP".

Geologic Settings

One example is from UHP microdiamond-bearing quartzofeldspathic lenses of "saidenbachite" in the gneiss-eclogite unit of the Saxonian Erzgebirge (Bohemian Massif) adjacent to the Saidenbach reservoir (Germany; 56.220° N, 45.886° E; e.g., Massonne, 2003). The rock contains plagioclase + quartz + phengite + paragonite + garnet + kyanite + rutile + apatite + zircon + graphite + microdiamond. It underwent partial melting (e.g., Massonne, 2003; Stoeckhert et al. 2009) and has been interpreted to be magmatic in origin (Massonne, 2003; Massonne and Fockenberg, 2012). Estimates for peak conditions (Variscan orogeny) range from

84 4–5 to 7–8 GPa (e.g., Hwang et al. 2000; Massonne, 2003) at temperatures of at least ~1000 ^{o}C,
85 possibly as high as 1400 ^{o}C (Massonne and Fockenberg, 2012).

86 The second example is classic felsic "Saxony granulite" from Röhrsdorf in the Variscan
87 Saxon Granulite Massif, Germany (e.g., O'Brien, 2006; Rötzler et al. 2008). The rock is finely
88 laminated due to a ribbon quartz foliation, whitish, and contains plagioclase + quartz + garnet +
89 kyanite + biotite + rutile + apatite + zircon. The rocks record eclogite facies conditions of 1000-
90 1050 ^{o}C and 2.2-2.3 GPa (e.g., Rötzler and Romer, 2001; Rötzler et al. 2008).
91 Following subduction, exhumation of both rocks occurred rapidly, largely under
92 ultrahigh-temperature conditions >900 ^{o}C (Rötzler et al. 2008; Stöckert et al. 2009; Massonne
93 and Fockenberg, 2012; Müller et al. 2015).

94 **Results**

95 The UHP Erzgebirge garnet preserves a striking increase in P content from core to rim,
96 followed by a narrow zone of low P at the outermost rim (Figs. 1a and 1b). The P zoning
97 between compositional domains ranges from somewhat diffuse in the core to sharp; the sharper
98 transitions dominate. The zones are roughly concentric, but they clearly overlap and cross-
99 cutting relationships are evident. In all cases of cross cutting, the zone closer to the rim transects,
100 and is thus younger than, the more interior zone. Sodium preserves a similar, although somewhat
101 more subdued zoning pattern (Fig. 1c). Ti zoning, in contrast, is much more diffuse, being
102 highest in the core and then dropping toward the rim (Fig. 1d). Major elements preserve very
103 broad compositional zoning that we infer has been heavily influenced by intracrystalline
104 diffusion (e.g., Ca and Mg; Figs. 1d and 1e).
105 The second example is a garnet in the HP granulite that preserves spectacular zoning. The
106 P_2O_5 concentrations are very high in the interior portions of the garnet (~0.5 wt.%; Table 1), and

drop toward the rim (Figs. 2a and 2b). The high-P core is transected by irregular, finger-like domains of lower P content (Table 1). In detail, these low-P domains clearly cut, and are thus younger than, pre-existing high-P garnet regions, including areas preserving relic oscillatory growth zoning (Fig. 2b). Islands of partially replaced or unreplaced material persist in the low-P domains. The boundaries between the high-P and low-P domains are extremely sharp. Faint radial crack-like features are preserved around a multiphase inclusion composed mostly of phengite and biotite. The zoning patterns of Na and Ti mimic those of P, but are slightly more diffuse, particularly for Ti (Figs. 2e and 2f). High-P and high-Na domains coincide spatially, as do the corresponding low-concentration domains. In contrast, low-P and low-Na correlate with high-Ti, and *vice versa*. Interestingly, the Na-Ti relations are antithetical to well-known coupled substitutions such as $NaTi^{VI}M^{2+}_{-1}Al_{-1}$ (e.g. Ringwood and Major, 1971; Hermann and Spandler, 2008; Auzanneau et al. 2010).

Major element zonation is considerably smoother than that for the trace elements. The highest Ca concentrations coincide with the region of sharply-defined P zonation, but no corresponding sharp Ca zonation is evident (Fig. 2b). Magnesium is largely flat, except for low-Mg halos around mica inclusions reflecting retrograde Mg-Fe exchange (Fig. 2c). Similar to the Erzgebirge example, we conclude that major element zonation has been strongly smoothed by diffusion. Calcium preserves somewhat more compositional structure than Mg, consistent with recent diffusion coefficient calibrations that show that Ca diffuses more slowly than Mg (Chu and Ague, 2015).

Discussion

One explanation for the P (and Na) zonation in the Erzgebirge example is multiple episodes of uncoupled dissolution followed by precipitation of rim overgrowths. While some

episodes of this type cannot be ruled out and may have occurred, we consider them unlikely to be responsible for the bulk of the zoning, as experiments and pseudosection modeling provide no evidence for such episodes along the probable pressure-temperature path (Massonne and Fockenberg, 2012).

The sharply-defined, overlapping, and cross-cutting chemical zonation patterns are also inconsistent with any simple growth or diffusion processes. They are consistent, however, with multiple ICDR events (Putnis and Austrheim, 2010; Putnis and John, 2010). In felsic, peraluminous systems, P and Na in garnet increase with pressure and temperature (e.g., Hermann and Spandler, 2008). Thus we interpret the core-rim increases in P and Na to trace progressively increasing metamorphic intensity during subduction to UHP conditions. Major elements do not record this, as their zonation has been heavily influenced by diffusion. Garnet may have been largely grown at relatively low metamorphic grades, and then progressively replaced by ICDR events with increasing subduction. The very low-P garnet rims developed during exhumation and cooling; they could reflect growth, ICDR, or some combination. Isolated fluid inclusions are present in garnet, but the interconnected porosity needed for ICDR is either at the nano scale and too small to observe optically, or was obliterated subsequent to ICDR.

Chemical profiles for P (Axler and Ague, 2015b) and the map (Fig. 2a) show some limited smoothing of zoning that almost certainly reflects diffusion, but the original abrupt transitions between compositional domains remain distinct. Sodium zoning is somewhat smoother than P, but still retains clear evidence for the compositional domains. As P and Na substitutions are likely coupled to some degree, it could be that the preservation of Na zoning is linked to extremely sluggish diffusion of P such that the two elements cannot move entirely independently. Titanium, however, exhibits much smoother zoning patterns, so it diffused more

readily than either P or Na in this setting (Fig. 1d). Nonetheless, small diffusional Ti depletion halos surround exsolved plates and needles of rutile. This relationship demonstrates that Ti for the rutile was locally sourced from garnet (e.g., Ague and Eckert, 2012; Axler and Ague, 2015b), and that the halos formed after most of the overall smoothing of Ti in garnet occurred.

The maximum P and Na contents measured by Axler and Ague (2015b; ~0.02–0.025 atoms per 12 O) correspond to pressure-temperature conditions of 700–800 ^{o}C and ~3–3.5 GPa according to the metapelite experiments of Hermann and Spandler (2008, their Fig. 4b). This is clearly UHP, but is not in the diamond stability field and the temperature is lower than current estimates (Massone and Fockenberg, 2012). These discrepancies likely reflect the need for more experimental data over a wide range of bulk compositions. In addition, as Na zoning is somewhat smoother than P, Na may have been lost preferentially, leading to anomalously low estimates. It is also possible that the highest-pressure parts of the garnet rim were modified by ICDR during the early stages of retrogression.

For the HP granulite, the extremely sharp, cross-cutting P zoning is once again consistent with ICDR, as is the near-isovolumetric replacement of the garnet crystal. The low-P and low-Na "fingers" are interpreted to have developed during retrogression while the garnet attempted to equilibrate to lower-P and lower-Na compositions at lower pressures and/or temperatures. Temperatures were likely still quite high, however, as major element zoning is largely smoothed and preserves no record of garnet replacement via ICDR. The radial, crack-like P zoning features around a micaceous multiphase inclusion probably reflect fluid-driven decrepitation during exhumation (e.g., Stöckhert et al. 2009). The interconnected nano-porosity for ICDR has either been destroyed or is not optically resolvable, although isolated fluid inclusions are present.

The maximum P_2O_5 content of the garnet is very high, approaching 0.5 wt.% (Table 1). This suggests UHP metamorphism given available experimental data; however, corresponding Na contents are not as high as observed by, e.g., Hermann and Spandler (2008), so we have not attempted a pressure estimate.

Implications

Complex zoning in garnet P, Na, and Ti may be preserved even in rocks that experienced extreme metamorphic conditions, and can record growth, diffusion, and both prograde and retrograde ICDR processes. Chemical mapping, as opposed to profiles, is essential to reveal the nature of this zoning. As ICDR is strongly associated with the presence of fluid (including melt), the core-to-rim increases in P and Na in garnet from UHP saidenbachite probably record successively deeper episodes of fluid-rock interaction on the prograde path during subduction, including the generation of partial melt at *T* possibly as high as 1400 ^{o}C (see Massonne and Fockenberg, 2012). In contrast, ICDR in the HP granulite, clearly illustrated by sharply-defined interpenetrating compositional domains, likely occurred during retrograde fluid-rock interaction. Major element zonation is strongly influenced by diffusion and is unable to record these histories. Diffusion of major elements almost certainly occurred simultaneously with ICDR across the advancing interface, and continued after cessation of ICDR.

Qualitatively, of the three elements, P diffused the slowest and Ti the fastest; given sufficient temperature and time, the Ti record of ICDR can be completely smoothed (Fig. 1d). It is likely that diffusion rates for the elements are not fully independent and are controlled to some extent by coupled substitutions such as $NaP\,M^{2+}_{-1}Si_{-1}$. The Ti contents of natural UHT and UHP garnets are commonly less than predicted by experiments (e.g., Hermann and Spandler, 2008; Ackerson et al. 2013). Thus, garnets probably lose Ti during retrogression; some of the escaping

Ti can be trapped as oriented rutile or ilmenite precipitates. Phosphorous and Na concentrations are also commonly lower than predicted. Local exsolution-related diffusion that forms apatite rods or plates can occur (e.g., Ye et al. 2000), and deformation may enhance their precipitation (e.g., Axler and Ague, 2015b). But for very slowly-diffusing elements like P, ICDR likely provides a much faster way of modifying crystal chemistry on a large scale (Figs. 1 and 2). Considerable work remains to determine trace element transport mechanisms in garnet, but tracer concentration systematics provide unique perspectives on processes operating at extreme conditions in the lithosphere.

Acknowledgements

We thank M.R. Ackerson and P.J. O'Brien for discussions, P.J. O'Brien for providing sample SB2 of diamondiferous saidenbachite, James O. Eckert, Jr., for EPMA assistance, L.P. Baumgartner, A. Putnis, and an anonymous referee for very constructive and helpful reviews, and the National Science Foundation Directorate of Geosciences (EAR-0744154, EAR-1250269) and Yale University and for support.

References Cited

Ackerson, M.R., Tailby, N., Watson, E.B. and Spear, F.S. (2013) Variations in Ti coordination and concentration in garnet in response to temperature, pressure and composition. American Geophysical Union Annual Meeting, San Francisco, California.

Ague, J.J. and Eckert, J.O., Jr. (2012) Precipitation of rutile and ilmenite needles in garnet: Implications for extreme metamorphic conditions in the Acadian orogen, USA. American Mineralogist, 97, 840-855.

Auzanneau, E., Schmidt, M.W., Vielzeuf, D. and Connolly, J.A.D. (2010) Titanium in phengite: a geobarometer for high temperature eclogites. Contributions to Mineralogy and Petrology, 159, 1-24.

Axler, J. A., and Ague, J. J. (2015a) Oriented multiphase needles in garnet from ultrahigh-temperature granulites, Connecticut, U.S.A. American Mineralogist. 100, 2254-2271.

Axler, J.A., and Ague, J.J. (2015b) Exsolution halos of rutile or apatite surrounding ruptured inclusions in garnet from UHT and UHP rocks. Journal of Metamorphic Geology, 33, 829-848.

Álvarez-Valero, A.M., Cesare, B., and Kriegsman, L.M. (2005) Formation of elliptical garnet in a metapelitic enclave by melt-assisted dissolution and reprecipitation. Journal of Metamorphic Geology, 23, 65-74.

Centrella, S., Austrheim, H., and Putnis, A. (2015) Coupled mass transfer through a fluid phase and volume preservation during the hydration of granulite: An example from the Bergen Arcs, Norway. Lithos, 236-237, 245-255.

Chen, Y.-X., Zhou, K., Zheng, Y.-F., Chen, R.-X., and Hu, Z. (2015) Garnet geochemistry records the action of metamorphic fluids in ultrahigh-pressure dioritic gneiss from the Sulu orogen. Chemical Geology, 398, 46-60.

Chu, X. and Ague, J.J. (2015) Analysis of experimental data on divalent cation diffusion kinetics in aluminosilicate garnets with application to timescales of peak Barrovian metamorphism, Scotland. Contributions to Mineralogy and Petrology, 170, doi:10.1007/s00410-015-1175-y.

Faryad, S.W., Klápová, H., and Nosál, L. (2010) Mechanism of formation of atoll garnet during high-pressure metamorphism. Mineralogical Magazine, 74, 111-126.

Geisler, T., Schaltegger, U., & Tomaschek, F. (2007). Re-equilibration of zircon in aqueous fluids and melts. Elements, 3, 43-50.

Geisler, T., Janssen, A., Scheiter, D., Stephan, T., Berndt, J., & Putnis, A. (2010). Aqueous corrosion of borosilicate glass under acidic conditions: a new corrosion mechanism. Journal of Non-Crystalline Solids, 356, 1458-1465.

Hames, W.E. and Menard, T. (1993) Fluid-assisted modification of garnet composition along rims, cracks, and mineral inclusion boundaries in samples of amphibolite facies schists. American Mineralogist, 78, 338-344.

Harlov, D.E., Wirth, R., and Hetherington, C.J. (2011) Fluid-mediated partial alteration in monazite: the role of coupled dissolution–reprecipitation in element redistribution and mass transfer. Contributions to Mineralogy and Petrology, 162, 329-348.

Hermann, J. and Spandler, C.J. (2008) Sediment melts at sub-arc depths: An experimental study. Journal of Petrology, 49, 717-740.

Hwang, S.-L., Shen, P., Chu, H.-T. and Yui, T.-F. (2000) Nanometer-size α-PbO_2-type TiO_2 in garnet: a thermobarometer for ultrahigh-pressure metamorphism. Science, 288, 321-324.

Jedlicka, R., Faryad, S.W., and Hauzenberger, C. (2015) Prograde Metamorphic History of UHP Granulites from the Moldanubian Zone (Bohemian Massif) Revealed by Major Element and Y+REE Zoning in Garnets. Journal of Petrology, doi: 10.1093/petrology/egv066.

Kawakami, T. and Hokada, T. (2011) Linking P-T path with development of discontinuous phosphorous zoning in garnet during high-temperature metamorphism – and example from Lutzow-Holm Complex, East Antarctica. Journal of Mineralogical and Petrological Sciences, 105, 175-186.

Kobayashi, T., Hirajima, T., Kawakami, T., and Svotjka, M. (2011) Metamorphic history of garnet-rich gneiss at Ktiš in the Lhenice shear zone, Moldanubian Zone of the southern Bohemian Massif, inferred from inclusions and compositional zoning of garnet. Lithos, 124, 46-65.

Mallmann, G., O'Neill, H St.C., Klemme, S. (2009) Heterogeneous distribution of phosphorus in olivine from otherwise well-equilibrated spinel peridotite xenoliths and its implications for the mantle geochemistry of lithium. Contributions to Mineralogy and Petrology, 158, 485-504.

Martin, L.A.J., Ballèvre, M., Boulvais, P., Halfpenny, A., Vanderhaeghe, O., Duchêne, S., and Deloule, E. (2011) Garnet re-equilibration by coupled dissolution–reprecipitation: evidence from textural, major element and oxygen isotope zoning of cloudy garnet. Journal of Metamorphic Geology, 29, 213-231.

Massonne, H.J. (2003) A comparison of the evolution of diamondiferous quartz-rich rocks from the Saxonian Erzgebirge and the Kokchetav Massif: are so-called diamondiferous gneisses magmatic rocks? Earth and Planetary Science Letters, 216, 347-364.

Massonne, H.J. and Fockenberg, T. (2012) Melting of metasedimentary rocks at ultrahigh pressure—Insights from experiments and thermodynamic calculations. Lithosphere, 4, 269-285.

Müller, T., Massonne, H.J., and Willner, A.P. (2015) Timescales of exhumation and cooling inferred by kinetic modeling: An example using a lamellar garnet pyroxenite from the Variscan Granulitgebirge, Germany. American Mineralogist, 100, 747-759.

Niedermeier D. R. D., Putnis A., Geisler T., Golla-Schindler U., and Putnis C. V. (2009) The mechanism of cation and oxygen isotope exchange in alkali feldspars under hydrothermal conditions. Contributions to Mineralogy and Petrology, 157, 65–76.

O'Brien, P.J. (2006) Type-locality granulites: high-pressure rocks formed at eclogite-facies conditions. Mineralogy and Petrology, 86, 161-175.

Page, F.Z., Essene, E.J., Mukasa, S.B., and Valley, J.W. (2013) A garnet-zircon oxygen isotope record of subduction and exhumation fluids from the Franciscan Complex, California. Journal of Petrology, 55, 103-131.

Pollok, K., Lloyd, G.E., Austrheim, H., and Putnis, A. (2008) Complex replacement patterns in garnets from Bergen Arcs eclogites: A combined EBSD and analytical TEM study. Chemie der Erde, 68, 177-191.

Putnis A. and Austrheim H. (2010) Fluid induced processes: Metasomatism and metamorphism. Geofluids, 10, 254-269.

Putnis A. and John T. (2010) Replacement processes in the Earth's crust. Elements, 6, 159-164.

Ringwood, A.E. and Major, A. (1971) Synthesis of majorite and other high-pressure garnets and perovskites. Earth and Planetary Science Letters, 12, 411-441.

Rötzler, J. and Romer, R.L. (2001) *P–T–t* evolution of ultrahigh-temperature granulites from the Saxon Granulite Massif, Germany. Part I: Petrology. Journal of Petrology, 42, 1995–2013.

Rötzler, J., Hagen, B., and Hoernes, S. (2008) Geothermometry of the ultrahigh-temperature Saxon granulites revisited. Part I: New evidence from key mineral assemblages and reaction textures. European Journal of Mineralogy, 20, 1097-1115.

Rubatto, D., Müntener, O., Barnhoorn, A., & Gregory, C. (2008). Dissolution-reprecipitation of zircon at low-temperature, high-pressure conditions (Lanzo Massif, Italy). American Mineralogist, 93, 1519-1529.

Spear, F. S. and Kohn, M. J. (1996) Trace element zoning in garnet as a monitor of crustal melting. Geology, 24, 1099–1102.

Stöckhert, B., Trepmann, C.A. and Massonne, H.-J. (2009) Decrepitated UHP fluid inclusions: About diverse phase assemblages and extreme decompression rates (Erzgebirge, Germany). Journal of Metamorphic Geology, 27, 673-684.

Vielzeuf, D., Veschambre, M., and Brunet, F. (2005) Oxygen isotope heterogeneities and diffusion profile in composite metamorphic-magmatic garnets from the Pyrenees. American Mineralogist, 90, 463-472.

Whitney, D.L. (1996) Garnets as open systems during regional metamorphism. Geology, 24, 147-150.

Xu, L., Xiao, Y., Wu, F., Li, S., Simon, K., and Wörner, G. (2013) Anatomy of garnets in a Jurassic granite from the south-eastern margin of the North China Craton: Magma sources and tectonic implications. Journal of Asian Earth Sciences, 78, 198-221.

Ye, K., Cong, B., and Ye, D. (2000) The possible subduction of continental material to depths greater than 200 km. Nature, 407, 734-736.

Figure Captions

Figure 1. Chemical maps of Erzgebirge garnet (sample SB2). Color scale ranges from blue to light yellow with increasing concentration. 500 μm scale bar. **(a)** Phosphorous. **(b)** Phosphorous, with successive cross-cutting compositional zones highlighted. There are at least six major compositional domains **(c)** Sodium. **(d)** Titanium. **(e)** Calcium. **(f)** Magnesium.

Figure 2. Chemical maps of HP granulite garnet (sample W12 4452). **(a)** Phosphorous. Note multiphase inclusion with radiating cracks (arrow). **(b)** Detail of boxed area shown in part (a). Note relic oscillatory growth zonation in northwestern part of garnet. **(c)** Calcium. **(d)** Magnesium. Note retrograde Mg depletion halos surrounding biotite inclusions. **(e)** Sodium. **(f)** Titanium.

This is a preprint, the final version is subject to change, of the American Mineralogist (MSA)
Cite as Authors (Year) Title. American Mineralogist, in press.
(DOI will not work until issue is live.) DOI: http://dx.doi.org/10.2138/am-2016-5707

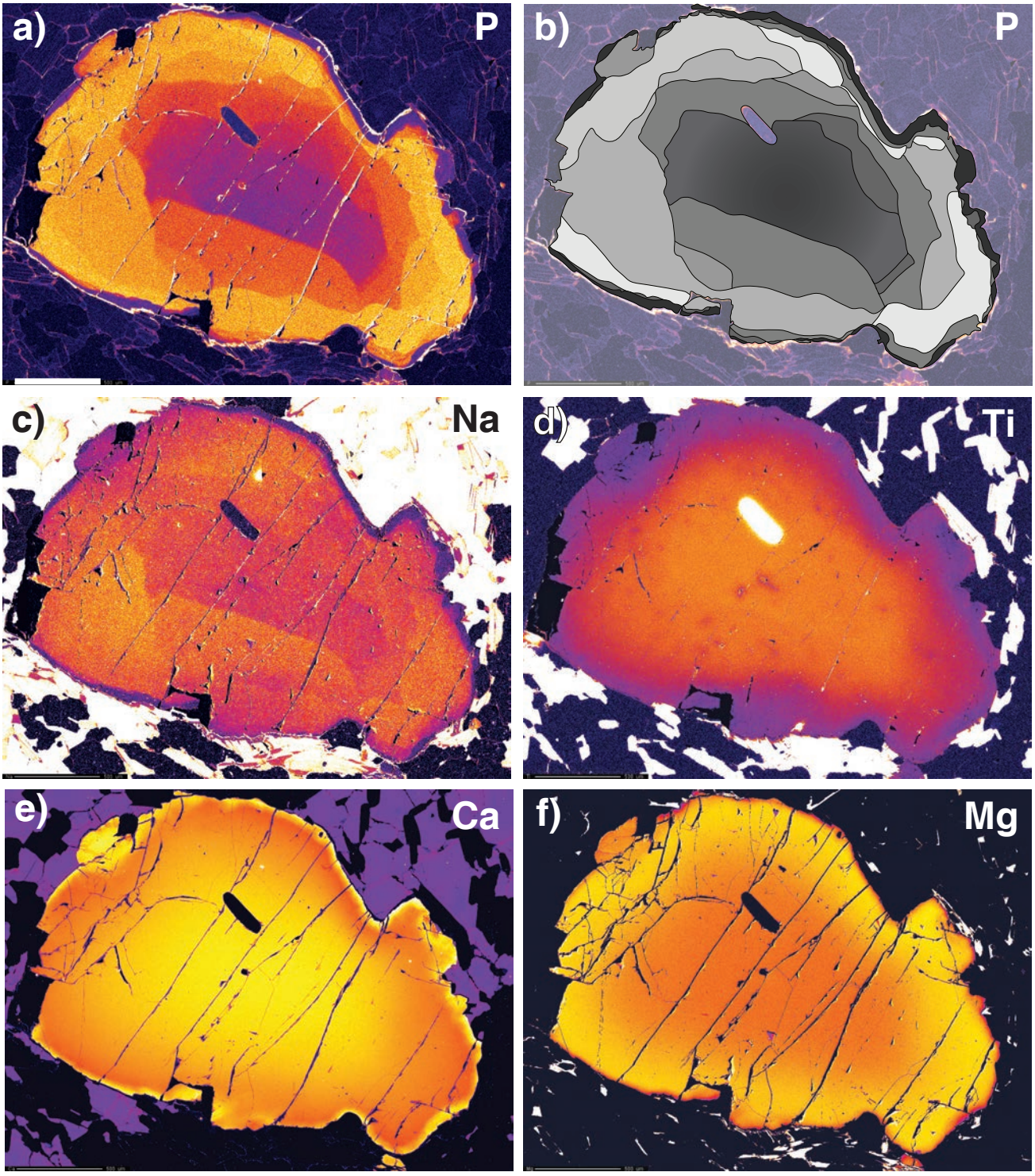

Ague and Axler, Figure 1

This is a preprint, the final version is subject to change, of the American Mineralogist (MSA)
Cite as Authors (Year) Title. American Mineralogist, in press.
(DOI will not work until issue is live.) DOI: http://dx.doi.org/10.2138/am-2016-5707

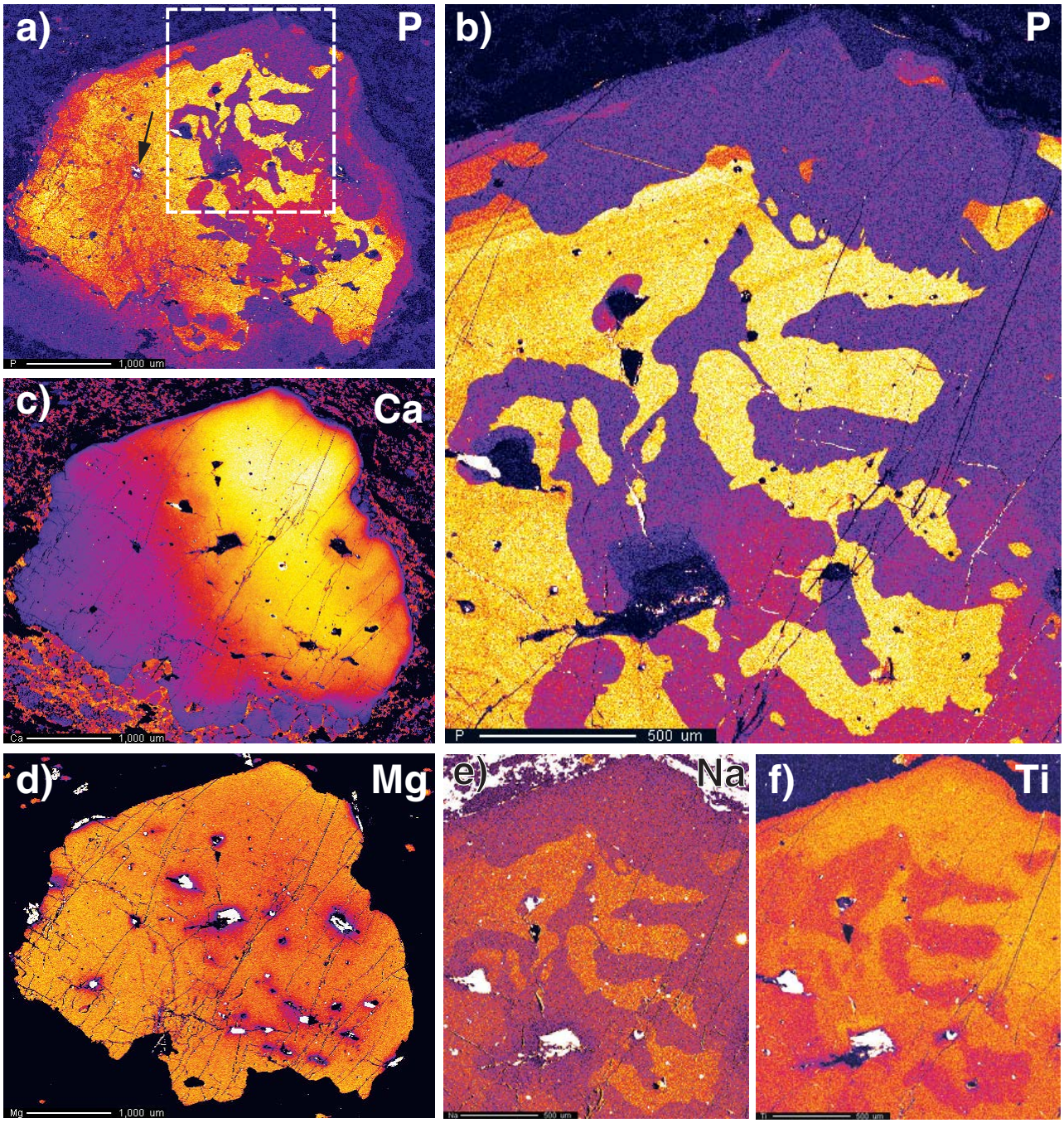

Ague and Axler, Figure 2

This is a preprint, the final version is subject to change, of the American Mineralogist (MSA)
Cite as Authors (Year) Title. American Mineralogist, in press.
(DOI will not work until issue is live.) DOI: http://dx.doi.org/10.2138/am-2016-5707

Table 1. Representative garnet analyses.

	Erzgebirge1 Low-Phosphorus Domain	**Erzgebirge2** High-Phosphorus Domain	**Saxony1** Low-Ca Domain	**Saxony2** High-Ca & High-Phosphorus Domain	**Saxony3** High-Ca & Low-Phosphorus Domain
	n=5	*n*=5	*n*=6	*n*=4	*n*=6
SiO_2	38.83(8)	38.73(1)	36.07(5)	36.18(5)	36.40 (6)
TiO_2	0.147(10)	0.020(3)	0.072(5)	0.076(8)	0.118(10)
P_2O_5	0.139(7)	0.340(2)	0.343(26)	0.479(7)	0.119(29)
Al_2O_3	21.97(2)	22.05(4)	20.67(3)	20.69(4)	20.63(6)
Cr_2O_3	0.01(<1)	0.01(<1)	b.d.	b.d.	b.d.
Y_2O_3	0.01(1)	b.d.	0.11(1)	0.08(1)	0.13(2)
FeO	27.00(5)	26.99(9)	39.68(10)	38.27(8)	38.37(14)
MgO	7.78(1)	8.13(9)	1.34(1)	1.24(2)	1.23(2)
MnO	0.29(1)	0.28(1)	0.94(2)	0.91(2)	0.91(2)
CaO	3.78(1)	3.50(13)	0.88(6)	2.30(7)	2.28(6)
Na_2O	0.102(6)	0.109(2)	0.039(3)	0.084(10)	0.041(4)
Total	100.05	100.17	100.19	100.36	100.31
			Structural Formulas (12 O)		
Si	2.994	2.979	2.949	2.944	2.965
Ti	0.0085	0.0012	0.0044	0.0047	0.0072
P	0.0091	0.0221	0.0237	0.0330	0.0082
Al	1.997	2.000	1.993	1.985	1.981
Cr	0.001	0.001			
Y			0.005	0.003	0.006
Fe^{3+}			0.030	0.030	0.049
Fe^{2+}	1.741	1.736	2.683	2.574	2.565
Mg	0.894	0.932	0.163	0.150	0.149
Mn	0.019	0.018	0.065	0.063	0.063
Ca	0.312	0.288	0.077	0.201	0.199
Na	0.0153	0.0163	0.0062	0.0133	0.0065

Notes: *b.d.* = below detection. *n* is the number of analyses averaged for each table entry. Fe^{2+} and Fe^{3+} in garnet estimated based on 8 cations per 12 O. The values in parentheses represent the 1σ uncertainties in the last digits.